Supporting information

Interlocking Dendritic Fibrous Nanosilica into Microgranules by Polyethylenimine Assisted Assembly: In-situ Neutron Diffraction and CO_2 Capture Studies

Jitendra Bahadur[1,2*], Swati Mehta[1,2], Saideep Singh[3], Avik, Das[1], Ayan Maity[3], Tristan Youngs[4], Debasis Sen[1,2], Vivek Polshettiwar[3*]

[1]Solid State Physics Division, Bhabha Atomic Research Centre, Mumbai, 400085, India

[2]Homi Bhabha National Institute, Anushaktinagar, Mumbai, 400094, India

[3]Department of Chemical Sciences, Tata Institute of Fundamental Research, Mumbai-400005, India

[4]Disordered Materials Group (ISIS), STFC Rutherford Appleton Laboratory, Oxfordshire, U.K.

1. Preparation and characterization of DFNS

In a typical synthesis procedure, urea and cetyltrimethylammonium bromide (CTAB) were dissolved in deionized (DI) water and stirred at 1400 rpm for 10 minutes. To the resultant mixture, a previously prepared solution of tetraethoxysilane (TEOS) in p-xylene/cyclohexane was added and stirring was continued for 10 minutes at 1400 rpm. Then, 1-pentanol (co-surfactant) was added drop wise to the final mixture and again stirred for 15 minutes. The resultant mixture was heated to require temperatures under refluxed conditions. After the completion of the reaction, the solid product was isolated by centrifugation and washed with ethanol and water several times followed by drying at 80°C for 8 hours. The product was then calcined at 550 °C for 6 h in (ramp rate 5°C/min) to obtain pure DFNS.

Name	Urea (g)	CTAB (g)	Water (ml)	Organic solvent (ml)	TEOS (ml)	Co-surfactant (ml)	Temperature (°C)	Heating Time (hours)
DFNS-L	12	10	500	500 (p-xylene)	100	30 (1-Pentanol)	130	2
DFNS-S	2.4	2	100	100 (cyclohexane)	5	6 (1-Pentanol)	90	12

Table-S1 Important synthesis parameters of the DFNS-S and DFNS-L

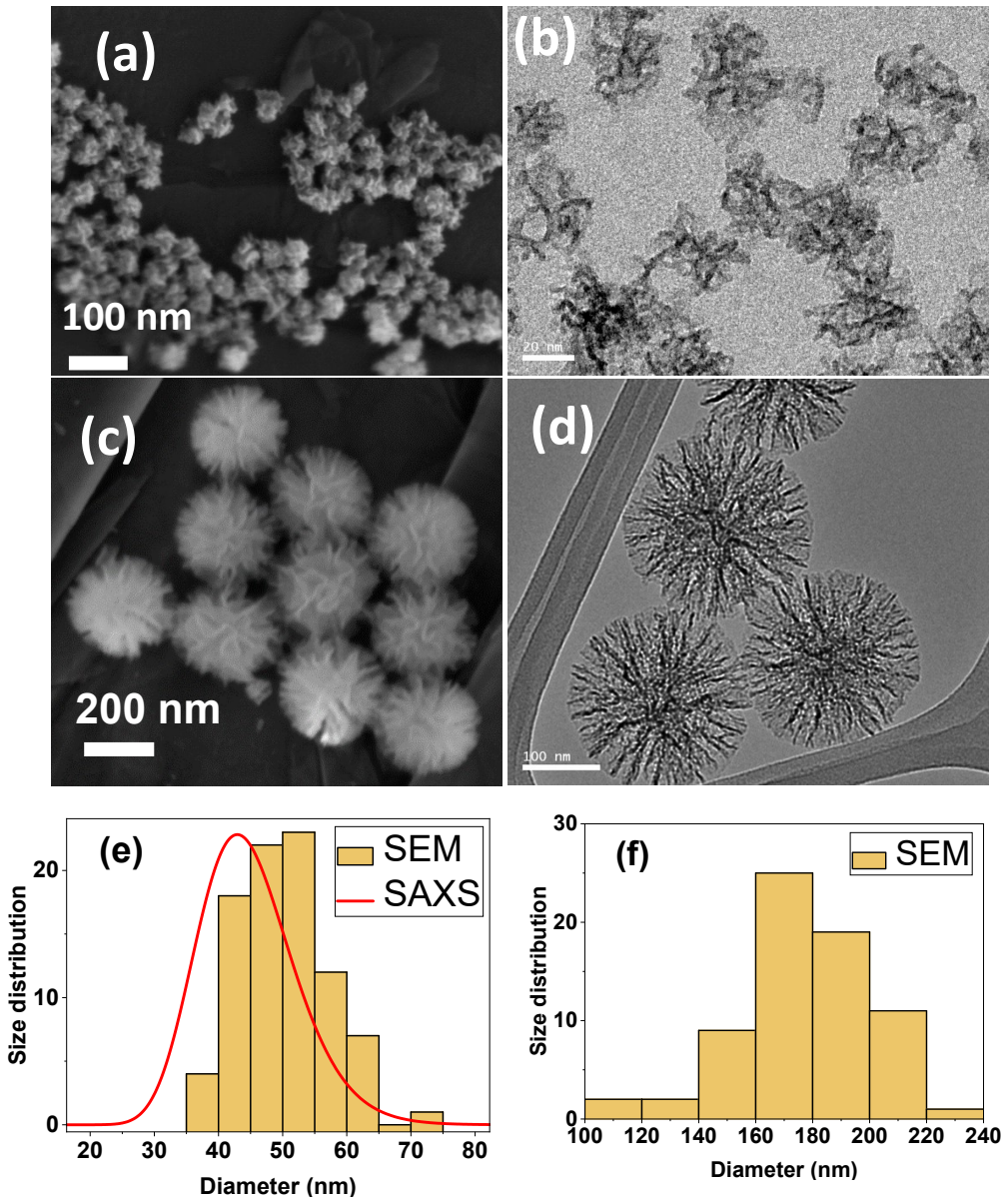

Fig. S1 *The (a, c) FESEM and (b,d) TEM micrographs of the DFNS-S (Top panel) and (Bottom panel) DFNS-L. Histogram of DFNS particle size (e) DFNS-S (f) DFNS-L*

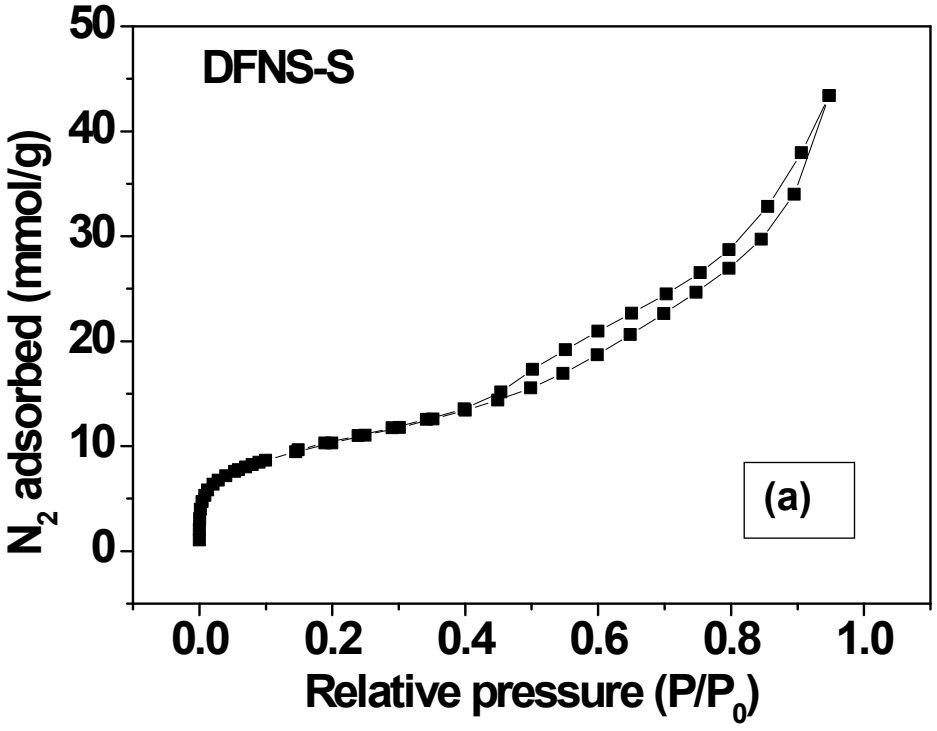
DFNS-S
(a)
N2 adsorbed (mmol/g)
Relative pressure (P/P0)
0
10
20
30
40
50
0.0
0.2
0.4
0.6
0.8
1.0

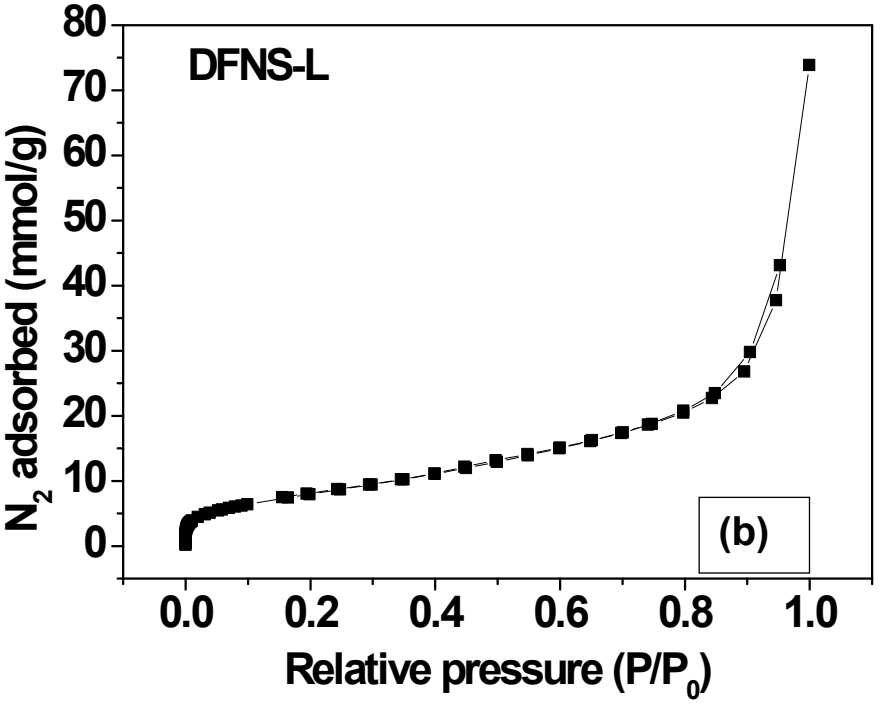
DFNS-L
(b)
N2 adsorbed (mmol/g)
Relative pressure (P/P0)
0
10
20
30
40
50
60
70
80
0.0
0.2
0.4
0.6
0.8
1.0

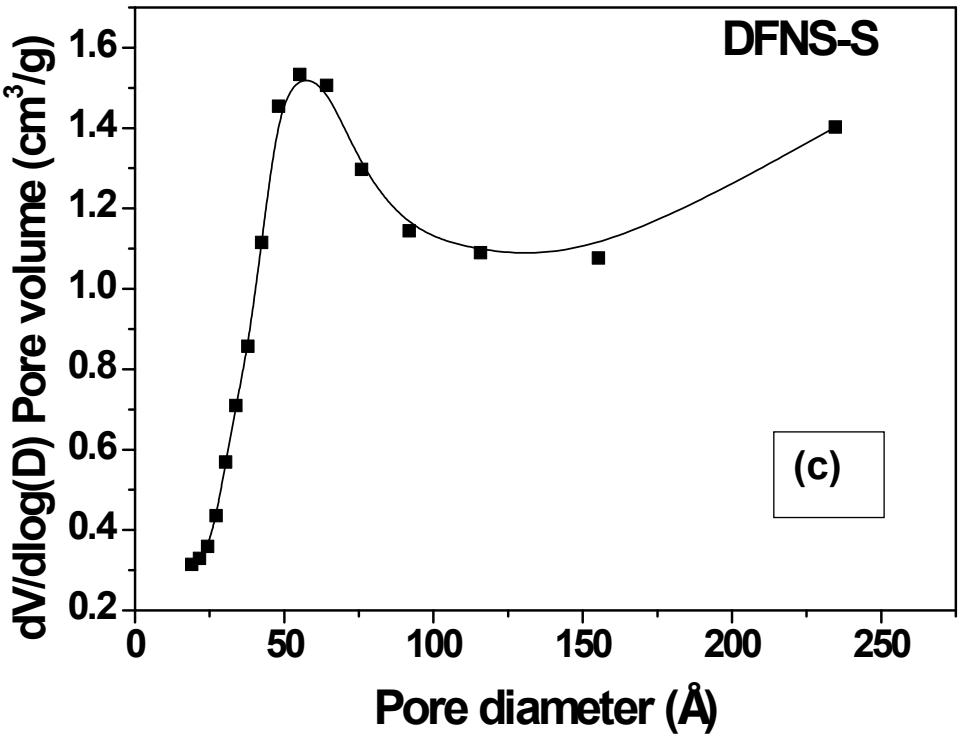
DFNS-S
(c)
dV/dlog(D) Pore volume (cm³/g)
Pore diameter (Å)
0.2
0.4
0.6
0.8
1.0
1.2
1.4
1.6
0
50
100
150
200
250

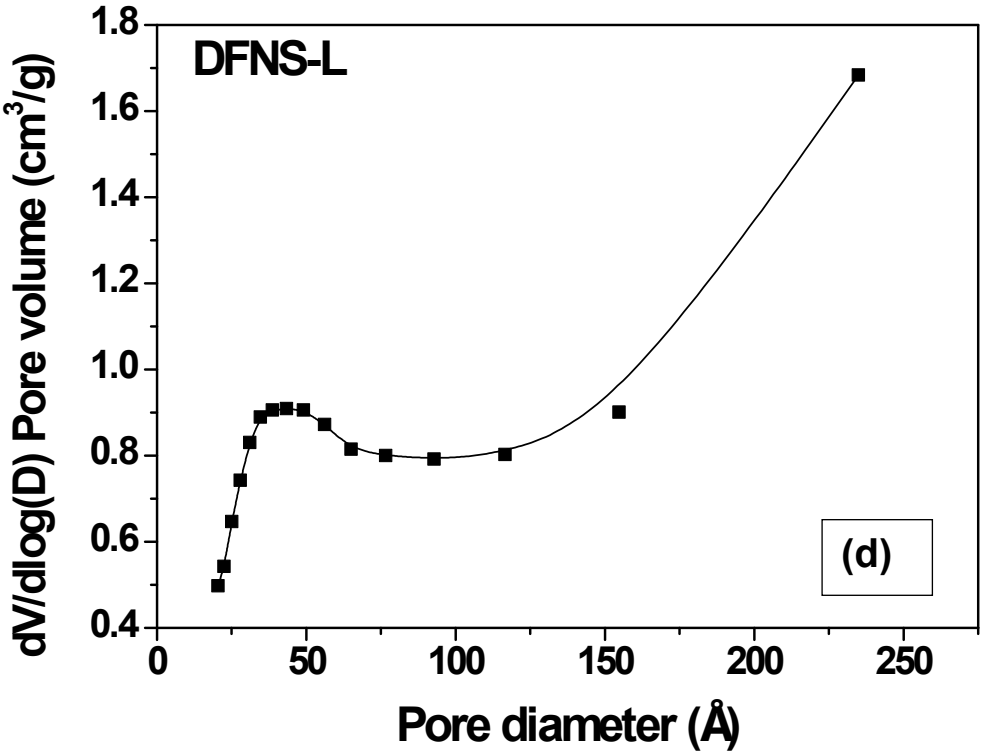
DFNS-L
(d)
dV/dlog(D) Pore volume (cm³/g)
Pore diameter (Å)
0.4
0.6
0.8
1.0
1.2
1.4
1.6
1.8
0
50
100
150
200
250

Fig. S2 *The N_2 adsorption isotherms (a,b) and pore size distributions (c,d) of DFNS-S and DFNS-L, respectively*

Table-S2 *The specific surface area and porosity before spray drying of the DFNS-S and DFNS-L particles*

Sample	BET surface area (m^2/g)	Pore volume (cm^3/g)
DFNS-S	841	1.4
DFNS-L	807	1.3

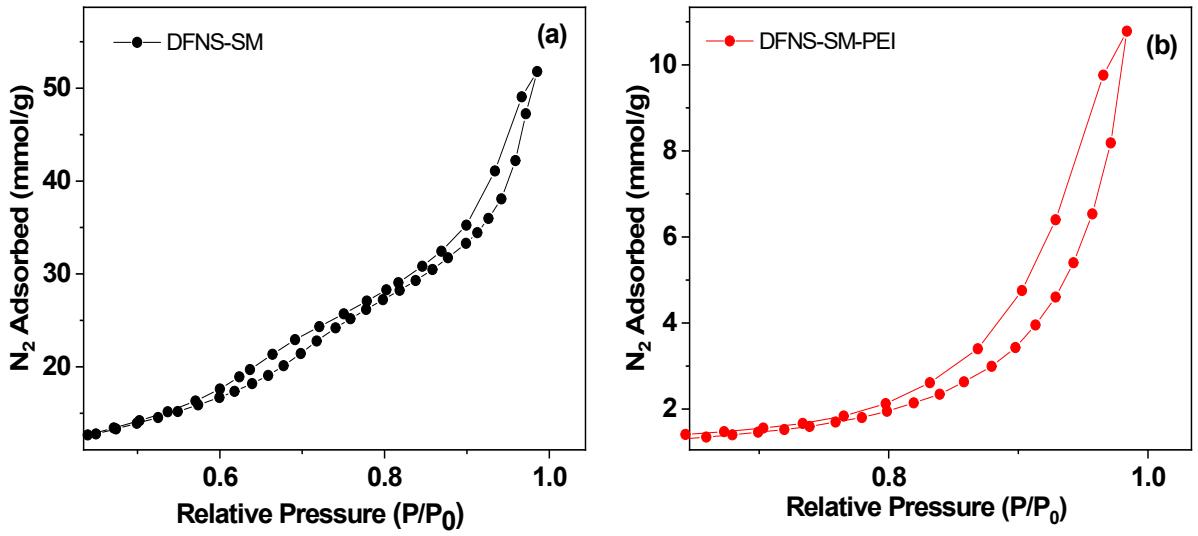

Figure S3: *Magnified image of N_2 adsorption isotherm and pore size distribution for DFNS-SM with and without PEI incorporation*

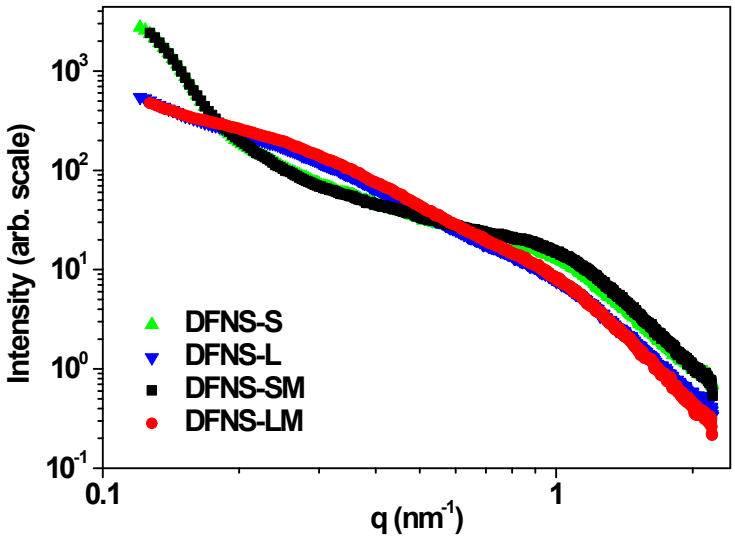

Figures S4 *The SAXS profiles of the DFNS particles before and after spray drying*

Fitting of the SAXS profile of DFNS microgranules:

$$I_{B\mu E}(q) = \langle \eta^2 \rangle \frac{8\pi\xi^2}{\left[1 + \left(\frac{2\pi\xi}{d}\right)^2\right]^2 + \left[-2\xi^2\left(\frac{2\pi\xi}{d}\right)^2 + 2\xi^2\right]q^2 + \xi^4 q^4} \qquad (1)$$

Here ξ is a correlation length beyond which the periodicity in the structure vanishes, whereas d is the periodic distance in the bicontinuous structure and represents the characteristics domain size. The pore structure in the bicontinuous structure depends on these characteristics length scales [1]. $\langle \eta^2 \rangle$ is the contrast factor and is defined as $\langle \eta^2 \rangle = \phi(1-\phi)\Delta\rho^2$. In the case of larger DFNS particles, a multi-level bicontinuous structure exists [1], for DFNS-L particles two-level bicontinuous structure model could fit the SAXS data in the entire experimental q-range as depicted in Fig. 4. For smaller DFNS-S, one level of bicontinuous structure is sufficient to fit the data quite well. The scattering signal from the DFNS not only contains the information of the intricate internal structure but also the overall DFNS particles. Therefore, the scattering

profiles has been modelled by taking into account additional contributions form DFNS as depicted below:

$$I(q) = I_{DFNS}(q) + \sum_{i=1}^{n} I^{n}{}_{B\mu E}(q) \qquad (2)$$

For the smaller DFNS-S particles, $I_{DFNS}(q)$ is modelled using the polydisperse sphere model, and lognormal pore distribution is assumed to account for the polydispersity. $I^{n}{}_{B\mu E}(q)$ is the scattering intensity from the n^{th} level of the bicontinuous structure. For DFNS-S, n=1 i.e., one level of bicontinuous structure fits the data. For larger size DFNS-L particles, n=2 i.e., two-level of the bicontinuous structure are necessary to fit the data. The experimental q-range was not sufficient to probe the particle size instead, a power-law scattering is considered to account for the surface scattering in the SAXS profiles.

Table S3 *SAXS profile fitting parameters*

Sample	**Level-1**			**Level-2**		
	Bicontinuous structure			DFNS scattering		
	$\langle\eta^2\rangle$	ξ (nm)	d (nm)	Median radius (nm)		Polydispersity index (σ)
DFNS-SM	0.37	1.6	16.3	22		0.18
DFNS-SM-PEI	0.32	1.6	16.3	19		0.25
	Bicontinuous structure-1			Bicontinuous structure-2		
	$\langle\eta^2\rangle$	ξ (nm)	d (nm)	$\langle\eta^2\rangle$	ξ (nm)	d (nm)
DFNS-LM	0.41	1.8	9.5	0.39	4.1	>100

DFNS-LM-PEI	0.08	1.8	10.0	0.20	14.7	>100

Table S4 *Comparison of CO_2 capture capacity in PEI based solid-adsorbents synthesized in the present work and PEI based solid adsorbents reported in the literature.*

Sorbent	**Temperature (℃)**	**CO_2 Pressure (bar)**	**Sorption capacity (mg/g)**	**Ref.**
DFNS-LM-PEI	75	1	105.6	This study
Silica gel-PEI(50)	75	1	78	[2]
SBA15-PEI(50)	75	1	89.8	[3]
SBA15-PEI(50)	75	5.5	95.4	[3]
I-SBA-15-PEI(50)	75	1	74.6	[4]
MCM41-PEI(30)	75	-	68.7	[5]
MCM41-PEI(50)	75	1	112	[5]
KCC1-PEI (LMW) (33wt%)	50	-	79.6	[6]
Fumed silica-PEI(33)	25	1	50.0	[7]
Fumed silica-PEI(50)	85	1	156	[8]

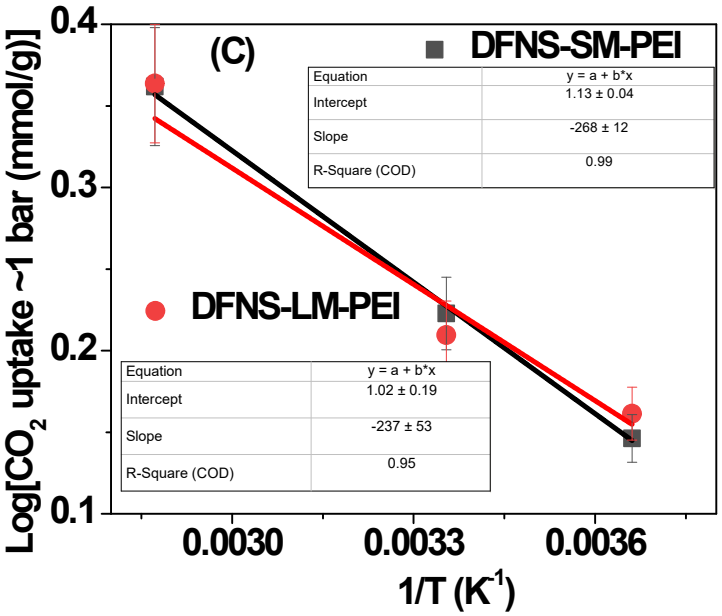

Fig. S5 *Temperature dependence of adsorption capacity at 1 bar along with linear fit.*

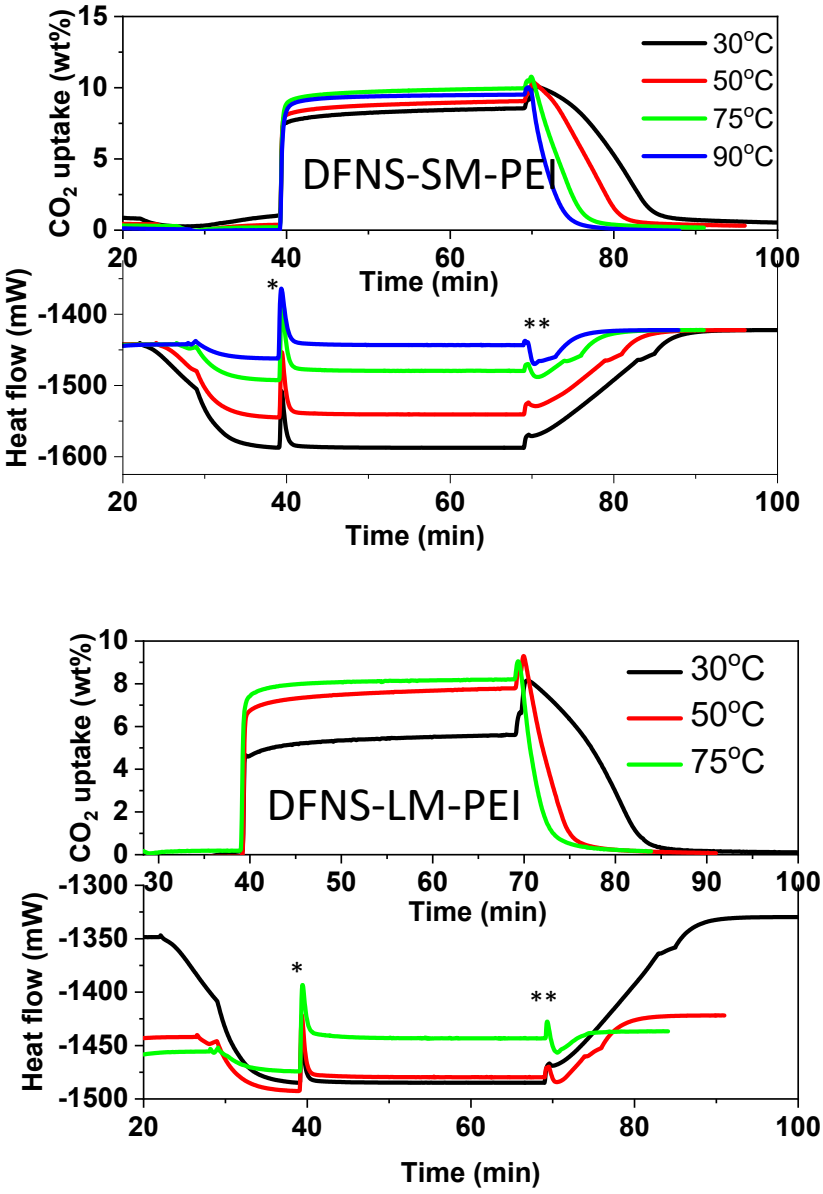

Figure S6 *CO_2 capture measured using thermogravimetric analysis under CO_2 flow for (a) DFNS-SM-PEI microspheres, and (b) DFNS-LM-PEI microspheres. CO_2 adsorption and desorption with time are illustrated. Further, exothermic peak due is also depicted as different adsorption temperature. The heat flow during the adsorption process is also depicted in differential thermogravimetric analysis (DTA) profiles. The adsorption and desorption peaks are marked* in * and ** in the DTA profile.

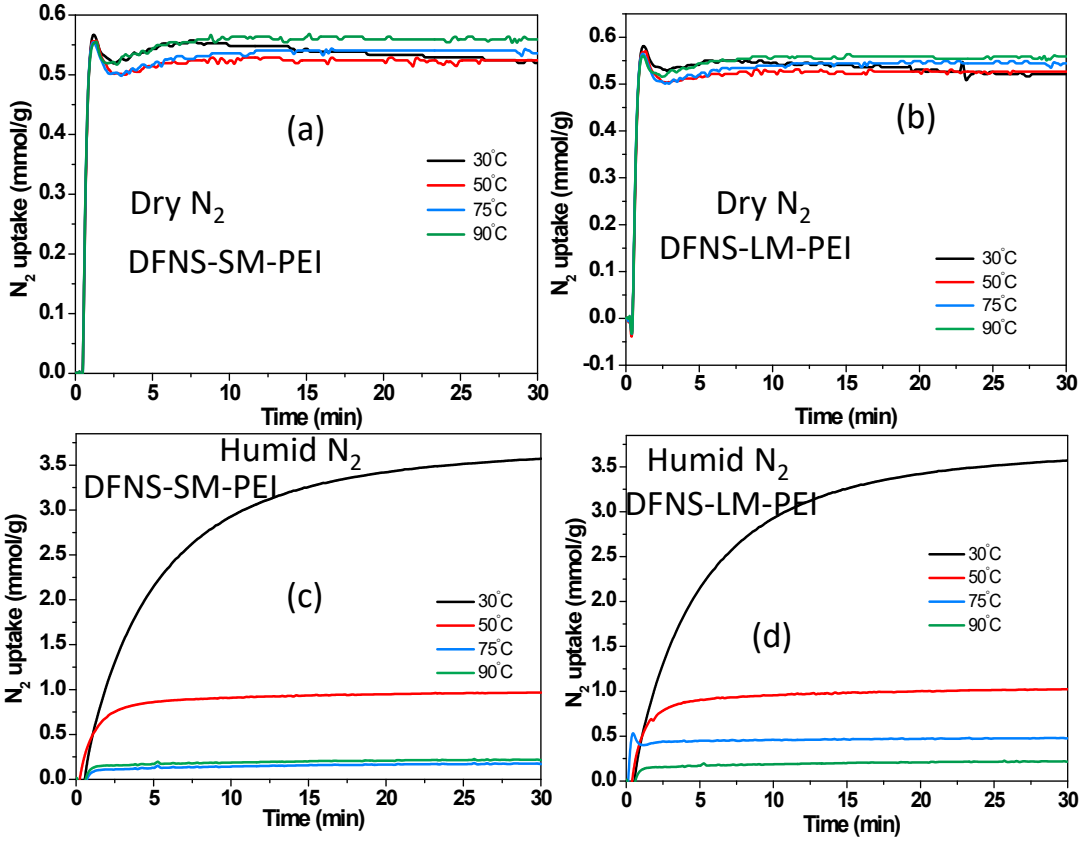

Fig. S7 *Thermogravimetric measurements under flow for DFNS-PEI microspheres for capture of (a,b) dry N_2 (c, d) Humid N_2 capture.*

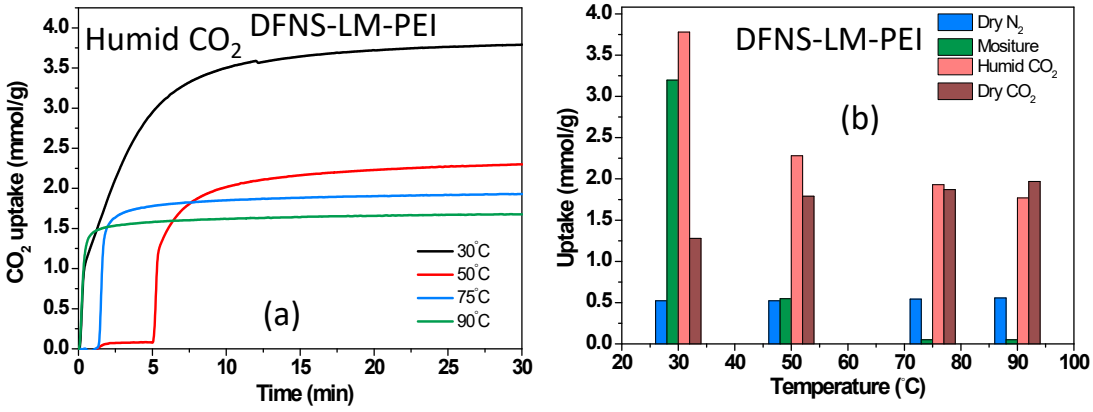

Fig. S8 (a) *Effect of moisture on CO_2 capture and* (b) *Capture capacity of N_2, H_2O (vapour) and CO_2 in PEI incorporated DFNS-LM-PEI microspheres*

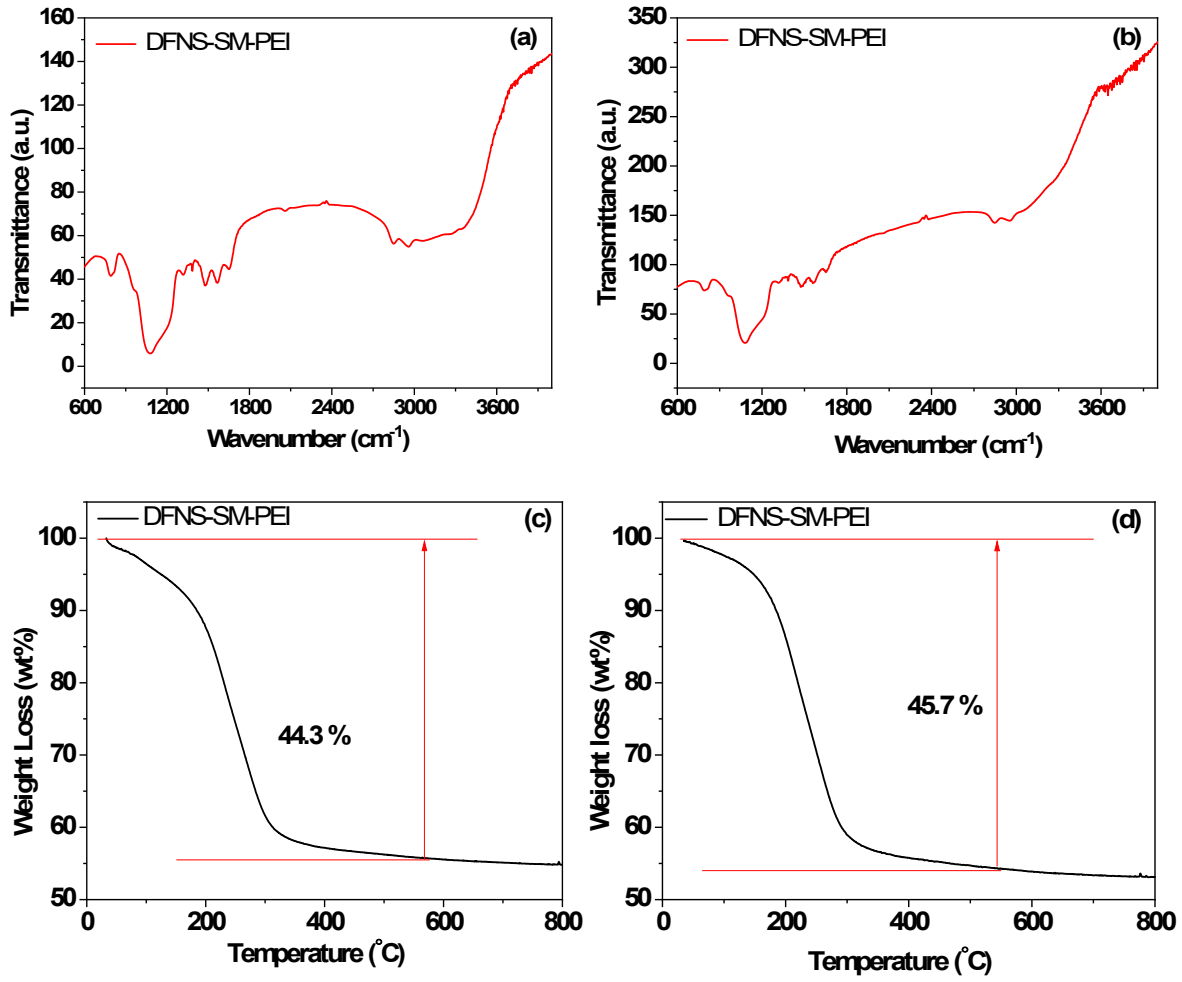

Figure S9: *FTIR spectra of DFNS-SM-PEI microgranules (a) before (b) after, TGA profile of DFNS-SM-PEI microgranules (c) before (d) after 50 regeneration cycles.*

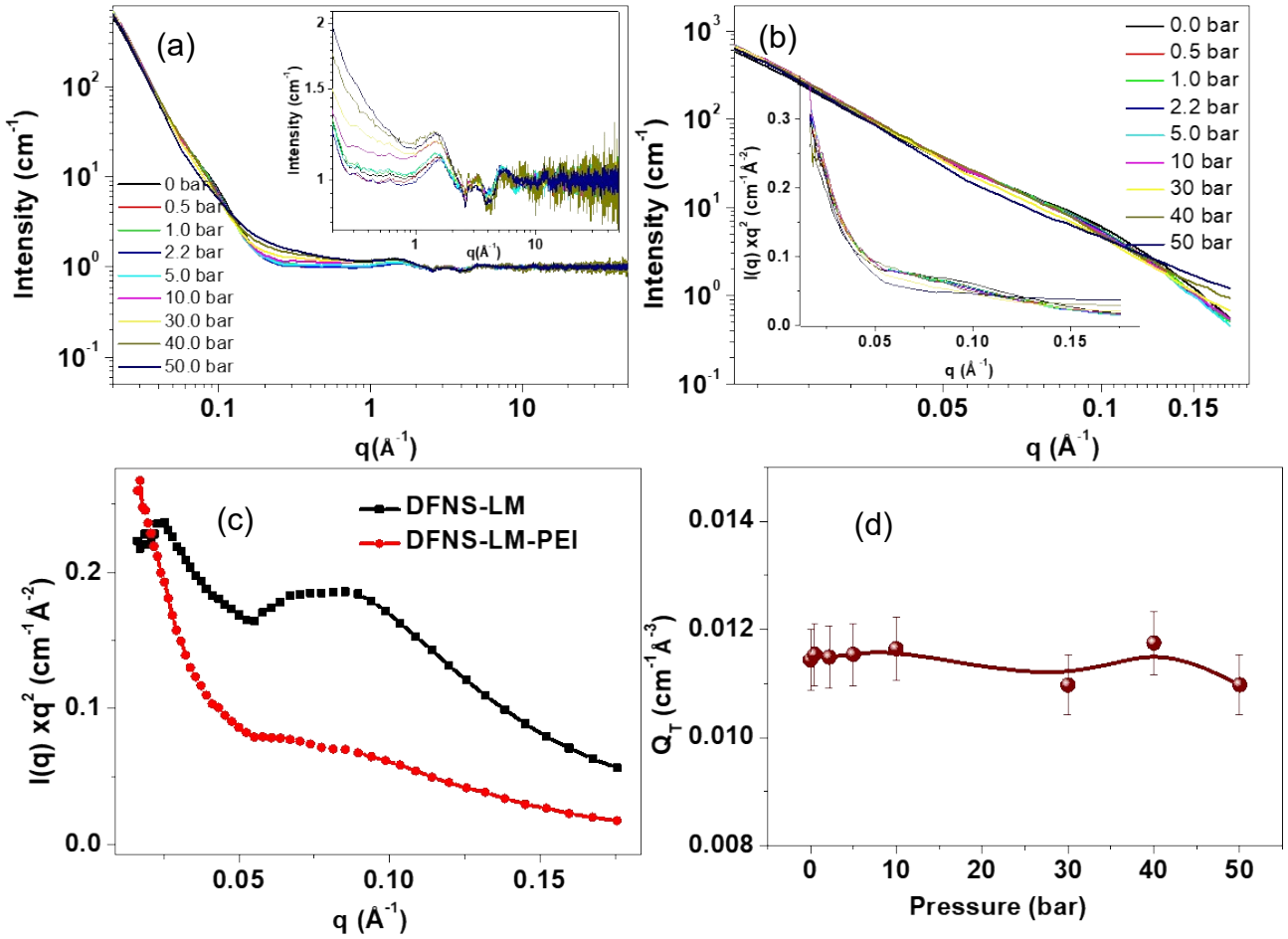

Figure S10 *In-situ neutron diffraction on the DFNS-LM-PEI microspheres as a function of CO_2 pressure (a) in the q-range of 0.02 to 50 Å^{-1}. Inset shows the zoom view of high-q data in the range of 0.20 to 50 Å^{-1}. (d) The comparison of the scattering data in the small-angle regimes for DFNS-LM and DFNS-LM-PEI microspheres. Scattering intensity is reduced significantly in the PEI incorporated microspheres due to the filling of the meso/macropores with PEI. (c) The scattering data in the small-angle regime in the range of 0.02 to 0.20 Å^{-1} is depicted. Inset shows the small-angle scattering data in the Kratky representation [I(q)q^2 vs. q] which shows two levels of meso and macropores. (d) The variation of the Porod invariant of the scattering data in the small-angle regime is shown as a function of pressure.*

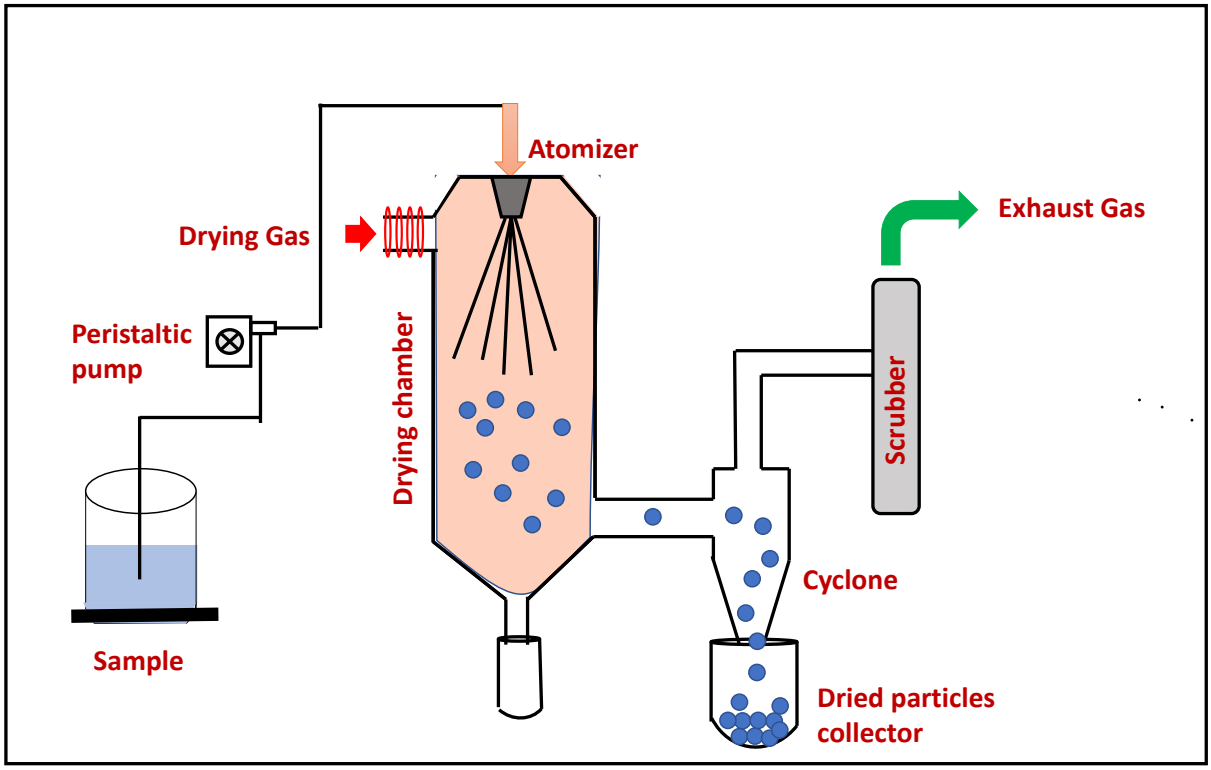

Schematic S1: *Spray dryer used for the realisation of DFNS-PEI microspheres.*

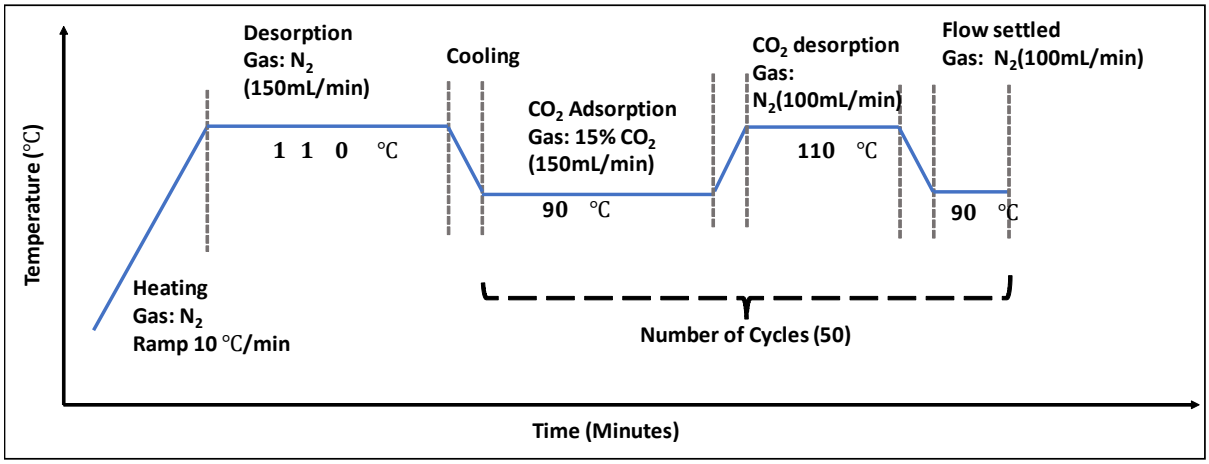

Schematic S2: *Schematic for the experimental method used in the CO_2 capture.*

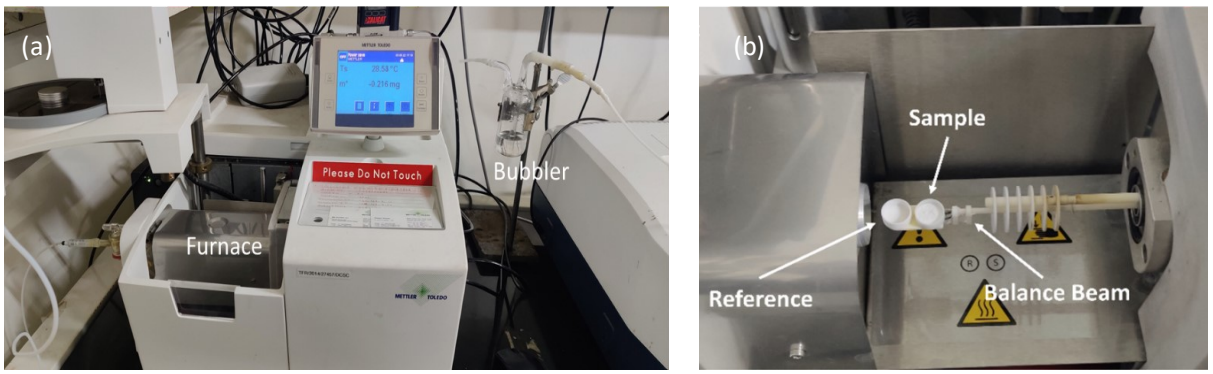

Figure S11: *Experimental set-up for the (a) TGA analysis with bubbler (b) Furnace and sample holder.*

References:

1. D. Sen, A. Maity, J. Bahadur, A. Das and V. Polshettiwar, *Microporous Mesoporous Materials*, 2021, 111234.
2. K. Li, J. Jiang, S. Tian, F. Yan and X. Chen, *Journal of Materials Chemistry A*, 2015, **3**, 2166-2175.
3. R. Sanz, G. Calleja, A. Arencibia and E. Sanz-Perez, *Applied Surface Science*, 2010, **256**, 5323-5328.
4. R. Sanz, G. Calleja, A. Arencibia and E. S. Sanz-Perez, *Microporous and mesoporous materials*, 2012, **158**, 309-317.
5. X. Xu, C. Song, J. M. Andresen, B. G. Miller and A. W. Scaroni, *Energy & Fuels*, 2002, **16**, 1463-1469.
6. B. Singh and V. Polshettiwar, *Journal of Materials Chemistry A*, 2016, **4**, 7005-7019.
7. A. Goeppert, H. Zhang, M. Czaun, R. B. May, G. S. Prakash, G. A. Olah and S. Narayanan, *ChemSusChem*, 2014, **7**, 1386-1397.
8. A. Goeppert, S. Meth, G. S. Prakash and G. A. Olah, *Energy & Environmental Science*, 2010, **3**, 1949-1960.